Chinese Journal of Natural Medicines

Epigallocatechin-3-gallate suppresses Hepatitis B virus replication through activating the AMPK/TFEB pathway to promote autophagic degradation of viral core protein

Yuling Yang, Di Yang, Yuxuan Yang, Zhe Wang, Lianhui Li, Maolong Wang, Jiayi Xu, Bingqiang Zhang, Lin Hou, Zibin Tian, Ning Li

Citation: Yuling Yang, Di Yang, Yuxuan Yang, Zhe Wang, Lianhui Li, Maolong Wang, Jiayi Xu, Bingqiang Zhang, Lin Hou, Zibin Tian, Ning Li, Epigallocatechin-3-gallate suppresses Hepatitis B virus replication through activating the AMPK/TFEB pathway to promote autophagic degradation of viral core protein, Chinese Journal of Natural Medicines, 2026, 24(3), 300-312. doi: 10.1016/S1875-5364(26)61105-3.

View online: https://doi.org/10.1016/S1875-5364(26)61105-3

Chinese Journal of Natural Medicines 24 (2026) 300-312

Contents lists available at ScienceDirect

Chinese Journal of Natural Medicines

journal homepage: www.cjnmcpu.com/

Original article

Epigallocatechin-3-gallate suppresses Hepatitis B virus replication through activating the AMPK/TFEB pathway to promote autophagic degradation of viral core protein

Yuling Yang[a,Δ], Di Yang[b,Δ], Yuxuan Yang[b], Zhe Wang[b], Lianhui Li[b], Maolong Wang[c], Jiayi Xu[b], Bingqiang Zhang[d,e], Lin Hou[b], Zibin Tian[f,*], Ning Li[b,*]

[a] *Department of Infectious Diseases, The Affiliated Hospital of Qingdao University, Qingdao University, Qingdao 266000, China*
[b] *School of Basic Medicine, Qingdao Medical College, Qingdao University, Qingdao 266071, China*
[c] *Thoracic Surgery Department, The Affiliated Hospital of Qingdao University, Qingdao University, Qingdao 266000, China*
[d] *Qingdao Restore Medical Laboratory Co., Ltd., Qingdao 266111, China*
[e] *Key Laboratory of Cancer and Immune Cells of Qingdao, Qingdao 266111, China*
[f] *Gastroenterology Department, The Affiliated Hospital of Qingdao University, Qingdao University, Qingdao 266000, China*

ARTICLE INFO

Article history:
Received 14 January 2025
Revised 13 April 2025
Accepted 17 April 2025
Available online 20 March 2026

Keywords:
EGCG
HBV
Autophagy
AMPK
TFEB
Lysosome biogenesis

ABSTRACT

Epigallocatechin-3-gallate (EGCG), a major polyphenolic compound in green tea, exhibits antiviral activity against multiple viruses, including hepatitis B virus (HBV). However, its role in HBV replication and the underlying mechanisms remain incompletely understood. In this study, we investigated the effects of EGCG on HBV replication and its modulation of autophagy using two established HBV cell models. Our results show that EGCG significantly reduces secreted levels of hepatitis B surface antigen (HBsAg) and HBV deoxyribonucleic acid (DNA), as well as intracellular HBV DNA replicative intermediates, encapsidated pregenomic ribonucleic acid (pgRNA), and core protein (HBc), without affecting total HBV messenger RNAs (mRNAs) or pgRNA levels. EGCG enhances autophagic flux, evidenced by increased autophagosome formation and accelerated turnover of the selective autophagy receptor p62 and LC3-Ⅱ. This enhanced autophagy promotes HBc degradation. Pharmacological inhibition of autophagy with 3-methyladenine (3-MA), chloroquine (CQ), or bafilomycin A1 (BafA1) abolished the suppressive effect of EGCG on HBV. Notably, treatment with CQ or BafA1 together with EGCG markedly increased HBV production by blocking autophagic degradation and inducing accumulation of autophagosomes—effects similar to those induced by the autophagy activator rapamycin, which facilitates HBV replication. Mechanistically, EGCG activates the adenosine 5'-monophosphate-activated protein kinase (AMPK)/transcription factor EB (TFEB) signaling axis, leading to enhanced lysosomal biogenesis and ATP production, thereby promoting autophagic clearance. Pharmacological or genetic inhibition of AMPK attenuated TFEB transcriptional activity, suppressed lysosomal biogenesis and ATP generation, impaired autophagic degradation, increased HBc levels, and ultimately enhanced HBV replication. Conversely, pharmacological activation of AMPK produced opposing effects. These findings reveal a novel mechanism by which EGCG inhibits HBV: EGCG promotes autophagic degradation of the viral core protein *via* activation of the AMPK/TFEB signaling pathway.

1. Introduction

Hepatitis B virus (HBV) infection poses a significant global health threat, leading to chronic, acute, and severe hepatitis, thereby increasing the risk of liver cirrhosis, liver failure, and even hepatocellular carcinoma and other end-stage liver diseases [1-3]. According to World Health Organization (WHO) statistics, approximately 250 million individuals worldwide live with chronic HBV infection, with more than 64% of cases concentrated in the Asia Pacific region. An estimated 2 billion people have been infected at some point, and nearly 1 million die annually from HBV-related complications [1, 3-6]. Current anti-viral therapies for chronic hepatitis B primarily rely on nucleos(t)ide analogs (NAs) and pegylated interferon (Peg-IFN) [7]. However, their clinical utility is limited by low cure rates, side effects, and drug resistance [8, 9], underscoring the urgent need for novel, safe, and effective anti-HBV agents.

In China and other regions, traditional Chinese medicines (TCMs) are frequently explored as potential treatments for hepatitis B due to their distinct anti-viral properties and additional therapeutic benefits [10, 11]. Among these, epigallocatechin-3-gallate (EGCG)—a catechin monomer derived from tea and a major component of tea polyphenols—exhibits a broad spectrum of biological activities, including anti-viral, anti-oxidative, anti-arteriosclerotic, anti-thrombotic, anti-angiogenic, anti-inflammatory, anti-tumor, anti-bacterial, and neuroprotective effects [12]. Previous experimental studies have demonstrated that EGCG effectively inhibits HBV replication [13-17]. Recent evidence suggests that

* Corresponding author.
E-mail addresses: tianzbsun@163.com (Z. Tian); ning-99@163.com (N. Li)
Δ These authors contributed equally to this work.

https://doi.org/10.1016/S1875-5364(26)61105-3

EGCG exerts many of these beneficial effects through regulation of autophagic flux, although the underlying mechanisms vary across cell types and disease contexts [18–21]. However, whether modulation of autophagic signaling contributes to its anti-HBV activity remains incompletely understood. Early studies indicate a bidirectional relationship between autophagy and HBV replication: HBV induces autophagosome formation but blocks autophagic completion, as the HBx protein impairs lysosomal degradative function by disrupting acidification [22]. This implies that functional, degradative autophagy is detrimental to HBV survival—a notion supported by findings that EGCG suppresses HBV replication by enhancing lysosomal acidity and autophagy [14]. Nevertheless, the precise regulatory effects of EGCG on autophagy and lysosomal acidification, and the mechanistic link to HBV inhibition, remain unclear.

In this study, we confirmed the inhibitory effect of EGCG on HBV replication using two HBV-producing cellular models and systematically investigated its impact on the HBV life cycle and autophagic processes. We found that EGCG significantly suppressed HBV replication by enhancing autophagic flux, leading to degradation of the viral core protein. Mechanistically, EGCG activated the adenosine 5'-monophosphate-activated protein kinase (AMPK)/transcription factor EB (TFEB) signaling pathway, promoting lysosomal biogenesis and ATP production, thereby augmenting autophagic degradation. These findings reveal a novel mechanism underlying EGCG-mediated suppression of HBV replication and provide a pharmacological foundation for the further development and clinical application of EGCG as an anti-HBV agent.

2. Materials and methods

2.1. Materials and agents

EGCG with a purity greater than 98% was purchased from Nantong Feiyu Biotechnology Co., Ltd. (Nantong, China). Other reagents and kits, along with their suppliers, were as follows: 0.02% trypsin digestion solution (Beyotime Biotechnology, Shanghai, China); methyl thiazolyl tetrazolium (MTT) kit (Beijing Solarbio Science & Technology Co., Ltd., Beijing, China); penicillin–streptomycin mixture (Beyotime Biotechnology, Shanghai, China); HBV real-time quantitative polymerase chain reaction (PCR) kit and HBV antigen detection enzyme-linked immunosorbent assay (ELISA) kit (Shanghai Kehua Biological Engineering Co., Ltd., Shanghai, China); supernatant HBV deoxyribonucleic acid (DNA) extraction kit (Takara Bio Inc. Japan); cytoplasmic HBV DNA extraction kit (Bioteke Corporation (WuXi) Co., Ltd., Wuxi, China); MG132, Compound C (C.C), Acadesine (AICAR), bafilomycin A1 (BafA1), and rapamycin (MedChemExpress, USA); chloroquine (CQ), 3-methyladenine (3-MA), and rabbit anti-LC3 polyclonal antibodies (Sigma-Aldrich, USA); mouse anti-β-actin and p62 polyclonal antibodies (Santa Cruz Biotechnology, USA); anti-p-AMPK and anti-ACCα (Cell Signaling Technology, USA); anti-mammalian target of rapamycin (mTOR), anti-p-mTOR, anti-p-p70S6K, anti-p-ULK1(Ser556), anti-TFEB, and anti-LAMP1 (Proteintech, Wuhan, China); anti-p-ACCα (ABclonal, Wuhan, China); monoclonal anti-HBcAg (Millipore, Billerica, MA); and polyclonal anti-core (Dako, Carpinteria, CA).

2.2. Cell culture

HepG2.2.15 and HuH-7 cells were obtained from the State Key Laboratory for Diagnosis and Treatment of Infectious Diseases, The First Affiliated Hospital, Zhejiang University School of Medicine. Cells were cultured in DMEM (Gibco) supplemented with 15% fetal bovine serum (Gibco) under standard conditions: 5% CO_2, 37 °C, and saturated humidity. The medium was further supplemented with 1% penicillin–streptomycin. Cells were maintained in the logarithmic growth phase and routinely tested for mycoplasma contamination.

2.3. Cell viability assay

The effect of EGCG on cell viability was assessed using an MTT assay. Cells were adjusted to a concentration of 1×10^5 cells/mL and seeded at 1×10^4 cells/well in 96-well plates. After 24 h, cells were treated with various concentrations of EGCG (0, 20, 40, 80, 160, or 320 μmol·L^{-1}) for 24 h, or with 20, 40, or 80 μmol·L^{-1} EGCG for different durations (12, 24, 48, or 72 h). Following incubation, the culture medium was removed, and cells were washed twice with phosphate-buffered saline (PBS). Then, 10 μL of MTT solution (dissolved in PBS) was added to each well, followed by 4 h of incubation. After removal of the supernatant, 150 μL of DMSO was added to dissolve the formed purple formazan crystals. Absorbance was measured at 490 nm using a microplate reader (Bio-Rad, USA). Relative cell viability was normalized to the vehicle control after background subtraction and expressed as the ratio of experimental group A490 to control group A490 [23]. Each concentration and time point was analyzed in triplicate.

2.4. Plasmid transfection and ribonucleic acid (RNA) interference

Transient transfections in HepG2.2.15 cells were performed using Lipofectamine 2000 (Invitrogen, Carlsbad, CA) according to an optimized protocol described previously [24]. Briefly, HepG2.2.15 cells were digested, suspended, and transfected with double amounts of GFP-LC3, GFP-mCherry-LC3, or GFP-mCherry-p62 plasmids (three gifts from Professor Wei Liu, School of Medicine, Zhejiang University) using Lipofectamine 2000 following the manufacturer's instructions. Transfected cells were visualized using a laser scanning confocal microscope (STELLARIS 5, Leica) equipped with a 63 × Plan Apochromat 1.4 NA objective [25]. HuH-7 cells were transfected with pcDNA3.0-1.3HBV plasmid (a gift from Professor Liu Wei, School of Medicine, Zhejiang University) using Lipofectamine 2000 according to the manufacturer's protocol. AMPK small interfering RNA (siRNA) pools targeting AMPKα1 and AMPKα2 (sequences: 5′-CCCUCAAUAUUUAAAUCCUUCUGUG-3′, 5′-GAAUAAUGAAUGAAGCCAA-3′, 5′-GCAUACCAUCUUCGUGUAAGA-3′, 5′-GAUG AUGAGCAUGUACCUA-3′) were purchased from Shanghai GenePharma Co., Ltd. and delivered into cells using Lipofectamine RNAiMAX (Thermo Fisher Scientific). Briefly, 1.3×10^5 cells per well in six-well plates were transfected with 20 pmol siRNA as per the manufacturer's guidelines. A nonspecific siRNA with no homology to mammalian genes served as a negative control. Cells were harvested after 48 h or following an additional 24 h of drug treatment.

2.5. Detection of HBV antigen

Cells were seeded in 6-well plates. After EGCG treatment, culture supernatants were collected and diluted 10-fold with PBS. Levels of hepatitis B e antigen (HBeAg) and hepatitis B surface antigen (HBsAg) were quantified using ELISA kits according to the manufacturer's instructions. Optical density (OD) was measured at 450 nm using a microplate reader. Relative expression levels of HBsAg and HBeAg were calculated using the formula provided in the kit manual. Each concentration was analyzed in triplicate.

2.6. HBV DNA analysis

Supernatants were collected for extracellular HBV DNA ex-

traction using TaqTM kit (TaKaRa)'s MiniBEST Viral DNA Extraction Kit. Intracellular HBV DNA was isolated as previously described [24]. Briefly, cells were lysed in lysis buffer (50 mmol·L^{-1} Tris-HCl, pH 7.4, 1 mmol·L^{-1} EDTA, 1% NP-40) at 4 °C for 15 min and centrifuged at 14 000 × *g* for 1 min to remove nuclei. Cytoplasmic fractions were then processed using a Cell DNA Extraction Kit according to the manufacturer's protocol to isolate intracellular HBV DNA. Extracted DNA was quantified *via* real-time PCR using an HBV diagnostic kit as per the manufacturer's instructions.

2.7. HBV RNA analysis

Total cellular RNA was extracted using Trizol (Invitrogen). Purified RNA was treated with RQ1 RNase-Free DNase (Promega, Madison, WI) to eliminate genomic DNA contamination prior to reverse transcription. Encapsidated HBV pregenomic RNA (pgRNA) was purified following established protocols [24]: capsids were precipitated with polyethylene glycol (PEG)-8000, and pgRNA was extracted from the resulting pellets using Trizol, followed by DNase treatment. For quantification, both total HBV RNA and encapsidated pgRNA were reverse-transcribed using M-MLV Reverse Transcriptase (Promega) and quantified by real-time PCR with a SYBR® Premix Ex Taq™ kit (TaKaRa) as previously described. GAPDH was used as an internal control to normalize HBV RNA levels. Primer sequences are listed in Table 1.

Table 1 Primers used for real-time PCR.

Gene name	Type	Sequence 5'-3'
HBV RNAs	forward	TCTCTGCAATGTCAACGACC
	reverse	CAGACCAATTTATGCCTACAGC
HBV pgRNA	forward	CCATACTGCACTCAGGCAA
	reverse	ACCTGCCTCGTCGTCTAAC
GAPDH	forward	GGAGCCAAAAGGGTCATCATCT
	reverse	AGGGGCCATCCACAGTCTTCT

2.8. Detection of cytoplasmic nucleocapsids

As previously described [26], HepG2.2.15 cells were lysed with 0.5 mL of TE buffer (10 mmol·L^{-1} Tris-HCl, 1.0 mmol·L^{-1} EDTA, pH 8.0) containing 1% NP-40 at 37 °C for 10 min. Cell debris and nuclei were removed by centrifugation, and the supernatant was supplemented with 6 μmol·L^{-1} $MgCl_2$ and 100 μg·mL^{-1} DNase I (NEB, USA) to digest cellular DNA. The resulting lysate was then separated on a 1% agarose gel. After electrophoresis for 2 h, capsids were directly transferred to a nitrocellulose membrane and detected by immunoblotting using an anti-core antibody (DAKO), with signals visualized *via* enhanced chemiluminescence.

2.9. Western blotting and immunofluorescence staining

Cells were harvested and lysed in RIPA lysis buffer supplemented with 1% (*V*/*V*) PMSF and phosphatase inhibitors. Protein concentrations were determined using a BCA protein assay kit. Equal amounts of protein from each sample were separated by SDS-PAGE and transferred onto PVDF membranes (Millipore). Membranes were blocked with 5% bovine serum albumin (BSA) in TBST for 2 h, followed by incubation with primary antibodies overnight at 4 °C. The following day, membranes were washed and incubated with peroxidase-conjugated secondary antibodies for 1 h at room temperature. Protein bands were detected using a high-sensitivity enhanced chemiluminescence kit (Monad, China), and band intensities were quantified using ImageJ 1.54 software. Immunofluorescence staining was performed according to our laboratory's established protocol [25] and observed under a laser scanning confocal microscope or a fluorescence microscope.

2.10. Determination of ATP Levels

In accordance with the manufacturer's instructions, intracellular ATP levels were measured using a commercial ATP detection kit (Abbkine, KTB1016). Absorbance values were recorded on a SpectraMax microplate reader, normalized to total cellular protein content, and expressed as a percentage of the control group.

2.11. Statistical analysis

Data were analyzed using GraphPad Prism 6.0 and are presented as mean ± standard deviation (SD) from three independent experiments. Pairwise comparisons were performed using the two-sample *t*-test, while differences among multiple treatment groups were assessed by one-way analysis of variance (ANOVA), with statistical significance set at $P < 0.05$.

3. Results

3.1. EGCG promotes the autophagic degradation of HBV core proteins to inhibit viral replication

To validate the anti-HBV activity of epigallocatechin gallate (EGCG) *in vitro*, HepG2.2.15 cells—a cell line with stable HBV DNA replication—and a transient HBV replication system in human hepatoma HuH-7 cells transfected with a 1.3-fold-over-length HBV replicon plasmid were employed. The cytotoxicity of EGCG toward HepG2.2.15 and HuH-7 cells was assessed using the MTT assay. EGCG reduced cell viability in a dose- and time-dependent manner (Figs. 1A and 1B, Figs. S1A and S1B). Treatment with EGCG at concentrations up to 40 μmol·L^{-1} for durations up to 24 h did not significantly affect HepG2.2.15 cell survival, whereas 80 μmol·L^{-1} EGCG for ≤ 24 h had negligible effects on HuH-7 cell viability. The impact of EGCG on HBV replication was initially evaluated by measuring secreted HBsAg in culture supernatants, extracellular HBV DNA, and intracellular nucleocapsid-associated HBV DNA replication intermediates (RIs). All three markers decreased in a dose- and time-dependent manner in HepG2.2.15 cells following EGCG treatment (Figs. 1C and 1D). Consistent with these findings, EGCG exhibited anti-viral activity in the transiently transfected HuH-7 model (Fig. S2A).

To further delineate the role of EGCG in the HBV life cycle, its effects on viral transcription and nucleocapsid assembly were examined. Levels of total HBV RNAs—including 3.5 kb mRNA/pgRNA (pre-genomic RNA), 2.4, 2.1, and 0.7 kb mRNAs—along with HBV pgRNA and encapsidated pgRNA, were quantified *via* quantitative reverse transcription PCR (qRT-PCR). Cytoplasmic nucleocapsids were isolated using native agarose gel electrophoresis and analyzed by immunoblotting. EGCG treatment for 24 h did not alter total HBV RNA or pgRNA levels (Figs. 1E and 1F, top panels), but significantly reduced encapsidated pgRNA in a dose- and time-dependent manner (Figs.1E and 1F, bottom panels). Consistently, EGCG markedly diminished nucleocapsid abundance in HepG2.2.15 cells (Fig. 1G). These observations suggest that either nucleocapsid assembly was impaired, their degradation was enhanced, or the stability of the core protein (HBcAg) was reduced. To investigate this, intracellular HBcAg levels were assessed and found to be significantly decreased upon EGCG treatment (Fig. 1H and Fig. S2B). Notably, pretreatment with BafA1, a late-stage autophagy inhibitor, prevented the decline in

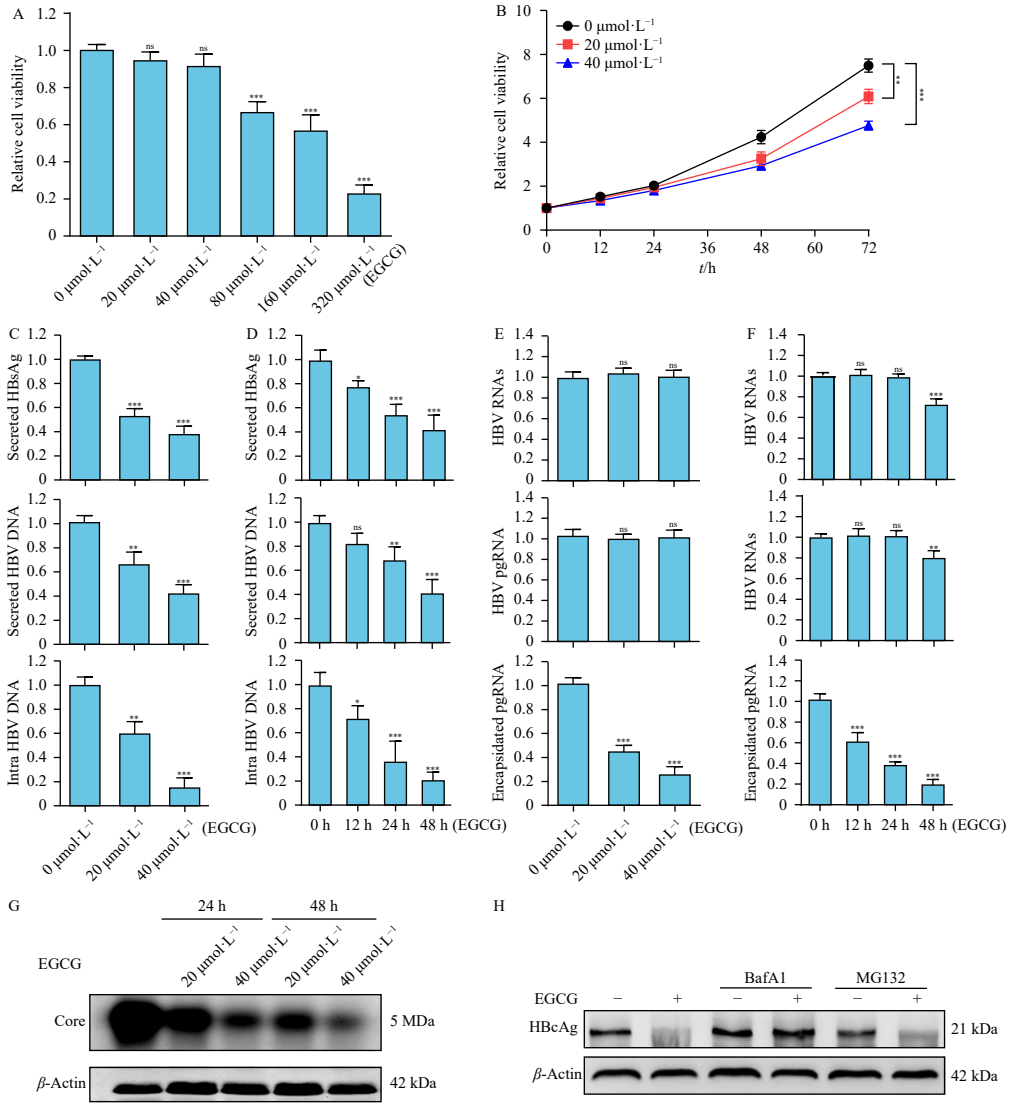

Fig. 1 The impact of EGCG on the HBV life cycle. (A) HepG2.2.15 cells were treated with the gradient doses of EGCG (0, 20, 40, 80, 160, 320 μmol·L^{-1}, respectively) for 24 h, and the cell viability was detected by MTT assay. (B) HepG2.2.15 cells were treated with 20 or 40 μmol·L^{-1} EGCG for 12 h, 24 h, 48 h, and 72 h, respectively, and the cell viability was detected. The values obtained from control samples were set at 1.0. Values are means ± SD (n = 5). (C–F) HepG2.2.15 cells were treated with different concentrations of EGCG for 24 h (C, E) or treated with 40 μmol·L^{-1} EGCG for varying durations (D, F), the levels of secreted HBsAg in the culture supernatants were measured by ELISA, the levels of secreted HBV DNA in the culture supernatants and intracellular HBV DNA RIs in the cytoplasm were measured by quantitative real-time PCR (qRT-PCR) (C, D), and the levels of total HBV RNAs, HBV pgRNA, and encapsidated pgRNA in the capsids were detected by qRT-PCR (E, F). The values obtained from the control group were set at 1.0. Data were presented as the means ± SD (n = 3). (G) HepG2.2.15 cells were treated with the different concentrations of EGCG for 24 h or 48 h. The cytoplasmic nucleocapsids were separated by agarose gel electrophoresis and detected by immunoblotting with the anti-core antibody. β-actin in the equal samples was assayed by Western blotting as an internal control. (H) HepG2.2.15 cells were left untreated (DMSO) or treated with EGCG (40 μmol·L^{-1}, 24 h) in the absence or presence of MG132 (10 μmol·L^{-1}) or bafilomycin A1 (BafA1, 100 nmol·L^{-1}). Intracellular HBcAg levels were determined by Western blotting with a specific anti-HBcAg antibody. ns means no significance. Data were analyzed using one-way ANOVA. $^{*}P < 0.05$, $^{**}P < 0.01$, $^{***}P < 0.001$ *vs* the 0 μmol·L^{-1} group or 0 h group.

HBcAg levels, whereas the proteasome inhibitor MG132 did not (Fig. 1H). This indicates that EGCG induces autophagic rather than proteasomal degradation of HBcAg. Collectively, these results demonstrate that EGCG suppresses HBV DNA replication through autophagic degradation of the viral core protein.

3.2. EGCG promotes autophagic flux in HBV-replicating cell models

The observation that EGCG induces autophagic degradation of HBV core protein prompted further investigation into its modulation of autophagy. HepG2.2.15 cells were transfected with a GFP-LC3 plasmid to monitor autophagosome formation *via* fluorescent puncta. EGCG treatment increased the number of GFP-LC3 puncta in a dose- and time-dependent manner, with Torin 1 serving as a positive control (Figs. 2A and 2B), indicating enhanced autophagosome formation. Endogenous LC3-II and p62—autophagy marker and cargo receptor, respectively—were analyzed by Western blotting. LC3-II levels increased while p62 levels decreased significantly in a dose- and time-dependent fashion upon EGCG exposure (Figs. 2C and 2D), suggesting enhanced autophagic flux. These effects were recapitulated in the 1.3-fold-HBV-transfected HuH-7 cells (Fig. S3). To assess dynamic autophagy, a GFP-mCherry-LC3 reporter was used. EGCG induced accumulation of LC3 puncta exhibiting strong mCherry but weak GFP fluorescence (Figs. 2E and 2F), indicative of autophagosome maturation and acidification, consistent with increased autophagic flux and cargo degradation in autolysosomes. Furthermore, co-treatment with BafA1 and EGCG led to greater accumulation of LC3-II and p62 compared to BafA1 alone (Fig. 2G), confirming that EGCG stimulates both autophagosome formation and downstream autophagic degradation in HBV-producing cells.

3.3. Autophagic degradation rather than autophagosome formation plays a key role in EGCG's inhibition of HBV replication

It has been reported that distinct stages of autophagy exert

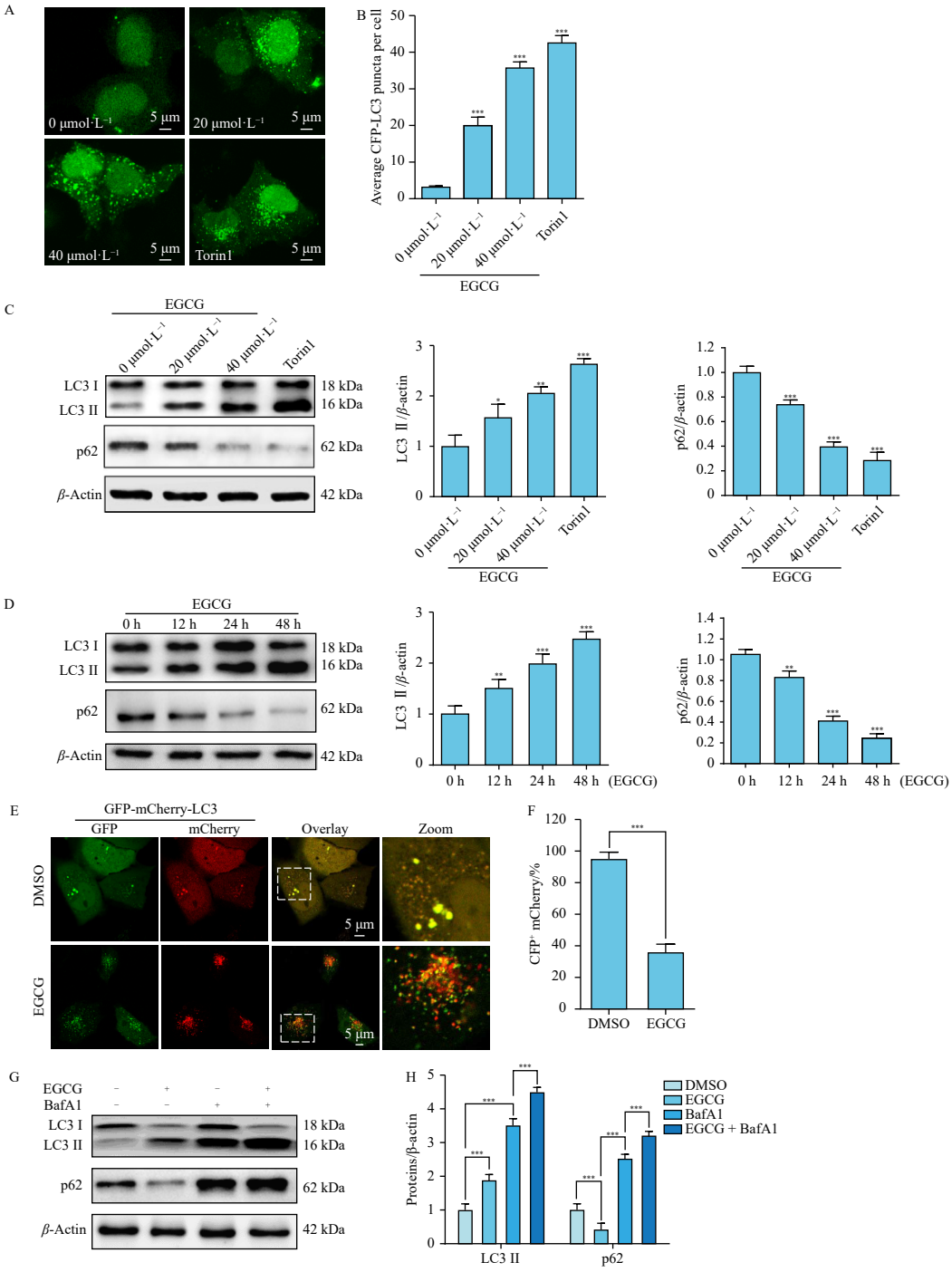

Fig. 2 EGCG enhances autophagic flux in HepG2.2.15 cells. (A, B) HepG2.2.15 cells transfected with GFP-LC3 were left untreated (DMSO) or treated with 20 or 40 μmol·L^{-1} EGCG for 24 h, or treated with 300 nmol·L^{-1} Torin1 for 4 h. The distribution of GFP-LC3 puncta was observed by confocal microscopy. Scale bars, 5 μm (A). The average count of GFP-LC3 puncta in cells was quantified with ImageJ (B). Values were means ± SD. n = 30 cells from three independent experiments. $^{***}P < 0.001$ *vs* the 0 μmol·L^{-1} group. (C, D) Western blotting analysis of endogenous LC3 and p62 levels in HepG2.2.15 cells treated with different concentrations of EGCG for 24 h (C) or treated with 40 μmol·L^{-1} EGCG for varying durations (D) and quantitative analysis of the blot bands of each protein with ImageJ. β-Actin was used as a loading control. The statistical results were presented as the means ± SD of three independent experiments. $^{*}P < 0.05$, $^{**}P < 0.01$, $^{***}P < 0.001$ *vs* the 0 μmol·L^{-1} group or 0 h group. (E, F) HepG2.2.15 cells transfected with GFP-mCherry-LC3 plasmid were treated with DMSO or 40 μmol·L^{-1} EGCG for 24 h. The distribution of mCherry and GFP puncta was examined by confocal microscopy and quantified with ImageJ. Scale bars, 5 μm. Values were means ± SD (n = 30). $^{***}P < 0.001$. (G, H) Western blotting analysis of endogenous LC3 and p62 levels in HepG2.2.15 cells untreated (DMSO) or treated with EGCG (40 μmol·L^{-1}) or BafA1 (100 nmol·L^{-1}) alone, or in a combination of both for 24 h. The blot bands were quantified by normalization to β-actin by ImageJ. Values were means ± SD (n = 3). Data in F were analyzed using two-sample t-test, and other data were analyzed using one-way ANOVA. $^{***}P < 0.001$.

opposing effects on HBV production: early autophagy supports viral DNA replication [27–30], whereas autophagic degradation negatively regulates it [22,31]. We therefore sought to determine whether the anti-HBV effect of EGCG depends on autophagic degradation. HepG2.2.15 cells were treated with EGCG in combination with either 3-MA—an inhibitor of autophagy initiation—or CQ, which blocks autophagosome-lysosome fusion. 3-MA significantly suppressed EGCG-induced GFP-LC3 puncta formation and LC3-II conversion (Figs. 3A–3C). Concomitantly, levels of secreted HBsAg, extracellular HBV DNA, and intracellular HBV DNA were higher in cells treated with EGCG plus 3-MA than with EGCG alone, although still below baseline levels in untreated controls (Fig. 3D), indicating partial reversal of EGCG's anti-viral effect and dependence on autophagy initiation. In contrast, CQ combined with EGCG dramatically increased GFP-LC3 puncta, LC3-II levels, and p62 accumulation (Fig. 3A–3C). Moreover, all

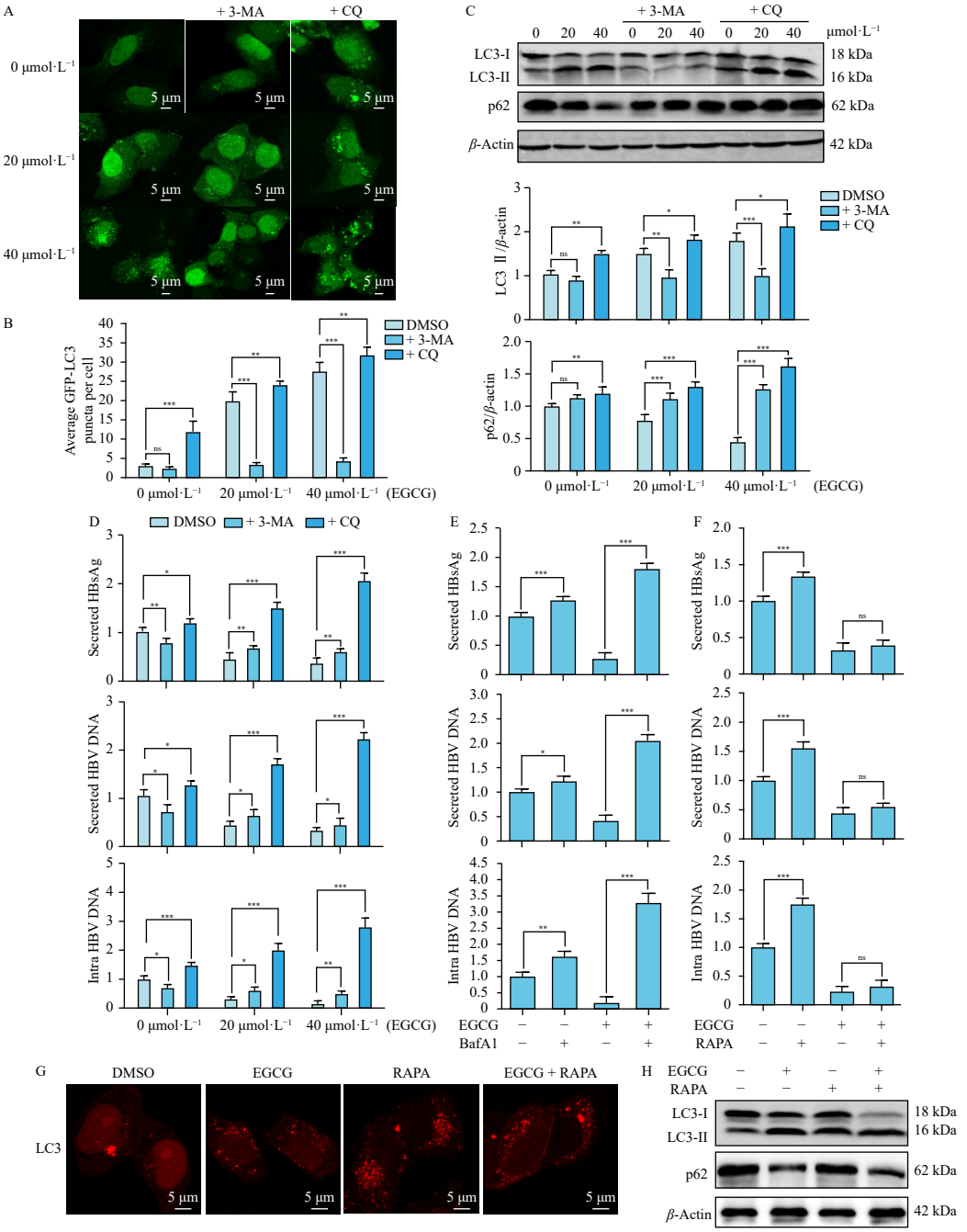

Fig. 3 Autophagic degradation, rather than the autophagosome formation induced by EGCG, suppresses HBV replication. (A–D) HepG2.2.15 cells transfected with GFP-LC3 were treated with DMSO or EGCG (20 or 40 μmol·L^{-1}) for 24 h after pretreatment for 1 h with autophagy inhibitor 3-MA (5 mmol·L^{-1}) or CQ (5 μmol·L^{-1}). The distribution of GFP-LC3 puncta was observed by confocal microscopy. Scale bars, 5 μm (A). The average count of GFP-LC3 puncta per cell was quantified from 30 cells from three independent experiments (B). The protein expressions of LC3 and p62 were detected by Western blotting and, the blot bands were quantified with ImageJ (C). The secreted HBsAg levels were detected by ELISA, and the secreted HBV DNA levels and the intracellular HBV DNA levels were determined by qRT-PCR (D). The values were normalized to those of the DMSO group and were presented as the means ± SD (n = 3). (E, F) HepG2.2.15 cells were either left untreated (DMSO) or treated with EGCG (40 μmol·L^{-1}, 24 h) alone, BafA1(100 nmol·L^{-1}, 24 h) alone, or in a combination of both (E). HepG2.2.15 cells were either left untreated (DMSO) or treated with EGCG (40 μmol·L^{-1}) alone, rapamycin (RAPA, 100 nmol·L^{-1}) alone, or in a combination of both for 24 h. Three indicators of HBV replication were detected as (D) described (F). (G, H) HepG2.2.15 cells were treated as (F) described. Cells were fixed, stained with the LC3 antibody, and observed by confocal microscopy. Scale bars, 5 μm (G). In parallel, the protein levels of LC3 and p62 in the cell lysates were analyzed *via* Western blotting (H). All experiments were repeated independently at least three times. ns means no significance. Data were analyzed using one-way ANOVA. $^{*}P < 0.05$, $^{**}P < 0.01$, $^{***}P < 0.001$.

three HBV replication markers were markedly elevated—exceeding even control levels—in an EGCG dose-dependent manner (Fig. 3D). Similar outcomes were observed when CQ was replaced with BafA1 in both HBV-producing cell lines (Fig. 3E and Fig. S2A). These findings indicate that blocking autophagic degradation or lysosomal fusion not only abrogates EGCG's inhibitory effect on HBV replication but also potentiates viral production. Notably, 3-MA alone suppressed autophagosome formation and HBV replication (Fig. 3D), whereas CQ or BafA1 alone promoted autophagosome accumulation (Figs. 3A and 3B) and enhanced HBV replication (Fig. 3D).

These data confirm that HBV replication relies on early autophagy and is abolished when autophagosome formation is inhibited. Conversely, late-stage autophagy—including autophagic degradation and autophagosome-lysosome fusion—negatively regulates HBV replication, likely through degradation of viral components. Thus, autophagic degradation, rather than autophagosome formation, is critical for EGCG-mediated suppression of HBV replication. To further validate this, we tested the autophagy inducer rapamycin (Figs. 3F and 3G). Rapamycin effect-

ively stimulated autophagosome formation and increased secretion of HBsAg, HBV DNA, and intracellular HBV DNA, yet failed to counteract EGCG's anti-viral effect (Fig. 3F and Fig. S2A). Western blotting analysis revealed that rapamycin alone did not reduce p62 levels, indicating incomplete autophagy, whereas co-treatment with EGCG enhanced LC3-II conversion and significantly decreased p62 (Fig. 3H). Together, these results indicate that incomplete or impaired autophagy promotes HBV replication, and that EGCG exerts its anti-HBV activity specifically by enhancing functional autophagic degradation.

3.4. EGCG activates the AMPK/TFEB signaling pathway and promotes lysosomal biogenesis and autophagic degradation

The above results underscore the importance of enhanced autophagic degradation in EGCG's anti-HBV activity. To further substantiate this, two complementary approaches were used. First, HepG2.2.15 cells were transfected with a GFP-mCherry-p62 plasmid to monitor autophagic flux. EGCG treatment significantly reduced the number of GFP-mCherry double-positive puncta (Figs. 4A and 4B), indicating efficient cargo delivery to acidic lysosomes. Second, a pulse-chase assay was performed to assess the turnover of preformed autophagosomes. While basal autophagosome degradation was slow in HepG2.2.15 cells, EGCG-treated cells exhibited accelerated degradation (Fig. 4C). To elucidate the underlying mechanism, the AMPK/mTOR signaling axis was examined by Western blotting. EGCG treatment increased phosphorylation of AMPK and its downstream targets—ACCα, ULK1, and TFEB (Fig. 4D and Fig. S3)—while decreasing phosphorylation of mTOR and its substrate p70S6K (Fig. 4D). Since mTOR-mediated ULK1 phosphorylation inhibits autophagy initiation, whereas AMPK-mediated ULK1 phosphorylation activates it, and since mTOR phosphorylates TFEB to retain it in the cytoplasm while AMPK activates TFEB's transcriptional function [32], our findings suggest that EGCG simultaneously inhibits mTOR and activates AMPK. Consequently, the AMPK/ULK1 axis may mediate autophagy initiation, while the AMPK/TFEB axis may drive autophagic degradation. Together, these pathways contribute to enhanced autophagic flux under EGCG treatment.

Consistent with the Western blotting data, immunofluorescence analysis revealed that EGCG induced nuclear translocation of TFEB (Fig. 4E), followed by upregulation of its target genes, including *TFEB* itself, *LAMP1* (encoding lysosome-associated membrane protein 1), and *ATP6V1A* (encoding a subunit of V-ATPase, essential for lysosomal acidification), as confirmed by qRT-PCR and immunostaining (Figs. 4E–4I). These results indicate that EGCG enhances TFEB transcriptional activity, thereby promoting lysosomal biogenesis and subsequent autophagic degradation. Additionally, ATP has been shown to activate lysosomal proteases and enhance degradative capacity [33]. Cellular ATP levels were significantly elevated in HepG2.2.15 cells after EGCG treatment (Fig. 4I), further supporting AMPK activation, as AMPK promotes catabolic processes and conserves cellular energy.

3.5. The enhancement of autophagic degradation and lysosomal biogenesis by EGCG depends on the activation of the AMPK/TFEB pathway

To determine whether AMPK mediates EGCG-induced autophagic flux and lysosomal biogenesis, pharmacological inhibition (C.C) and genetic knockdown (siRNA) of AMPK were employed. C.C treatment markedly reduced EGCG-induced AMPK phosphorylation (Fig. 5A). However, both C.C alone and in combination with EGCG, as well as AMPK knockdown, resulted in increased LC3-II and p62 accumulation (Figs. 5A, 5E, and S4) in both HBV-producing cell lines, accompanied by increased GFP-LC3 puncta (Fig. S5A), indicating impaired autophagic degradation. Using the GFP-mCherry-p62 reporter and pulse-chase assay, C.C treatment significantly increased double-positive puncta in EGCG-treated cells (Figs. 5B–5D), while AMPK knockdown nearly abolished degradation of EGCG-induced autophagosomes (Fig. 5D). Furthermore, AMPK knockdown attenuated EGCG-induced expression of TFEB and its targets *LAMP1* and *ATP6V1A*, as confirmed by Western blotting (Fig. 5E and Fig. S4), immunofluorescence staining (Figs. 5G–5J), and qRT-PCR (Fig. S6). Similar reductions in TFEB and LAMP1 signals were observed with C.C co-treatment (Figs. 5G–5J). Additionally, both C.C and AMPK knockdown significantly suppressed EGCG-induced ATP production (Fig. 5F and Fig. S7), providing another mechanism for impaired autophagic degradation.

Notably, although C.C or siAMPK treatment reduced EGCG-induced TFEB expression, nuclear localization of TFEB remained largely unaffected (Fig. 5G). This aligns with the observation that C.C had minimal effect on EGCG-induced mTOR inactivation (Fig. S8). Given that mTOR inactivation promotes TFEB nuclear translocation, while AMPK phosphorylation enhances its transcriptional activity, these findings suggest that EGCG modulates AMPK and mTOR independently, with mTOR inhibition occurring independently of AMPK. Collectively, these results demonstrate that the AMPK/TFEB signaling pathway mediates EGCG-induced autophagic degradation and lysosomal biogenesis.

3.6. EGCG inhibits HBV production by activating AMPK to promote the autophagic degradation of the HBV core protein

To determine whether AMPK-dependent autophagic degradation underlies the anti-HBV effects of EGCG, pharmacological and genetic interference with AMPK activity was applied. C.C treatment alone or in combination with EGCG significantly increased secreted HBsAg, extracellular HBV DNA, and intracellular HBV DNA in HepG2.2.15 cells, exceeding baseline replication levels (Fig. 6A). This indicates that EGCG's anti-viral effect is substantially attenuated and that AMPK inactivation promotes HBV replication. Similarly, AMPK knockdown alone or with EGCG markedly elevated all three HBV replication markers in both cell models (Fig. 6B and Fig. S9A) and restored HBcAg levels (Fig. 6D and Fig. S9B). In contrast, treatment with the AMPK activator AICAR strongly suppressed HBV replication (Fig. 6C) and enhanced autophagic degradation of HBcAg (Fig. 6E and Fig. S10). Notably, combining AICAR and EGCG showed no synergistic effect (Figs. 6C and 6E). These findings collectively indicate that AMPK-dependent autophagic degradation is essential for EGCG's anti-HBV activity.

4. Discussion

The present study comprehensively analyzed the regulation of EGCG on autophagy signaling and its effects on the HBV life cycle. In two cell models of HBV production, we found for the first time that EGCG did not affect HBV mRNA and pgRNA transcription but induced the autophagic degradation of the HBV core protein. This was accompanied by a reduction in nucleocapsids and encapsidated pgRNA, leading to decreased HBV-DNA synthesis and antigen secretion. Furthermore, we demonstrated that the anti-HBV effect of EGCG was mediated specifically by autophagic degradation rather than autophagosome formation. When autophagic degradation was blocked, EGCG-induced accumulation of autophagosomes significantly enhanced HBV production. Additionally, we showed that EGCG activated the AMPK/TFEB signaling pathway to promote lysosomal biogenesis and ATP production, thereby enhancing autophagic degradation of the HBV core protein (Fig. 7). These findings further support a previous study showing that EGCG inhibits HBV replication by enhancing lysosomal acidification [14].

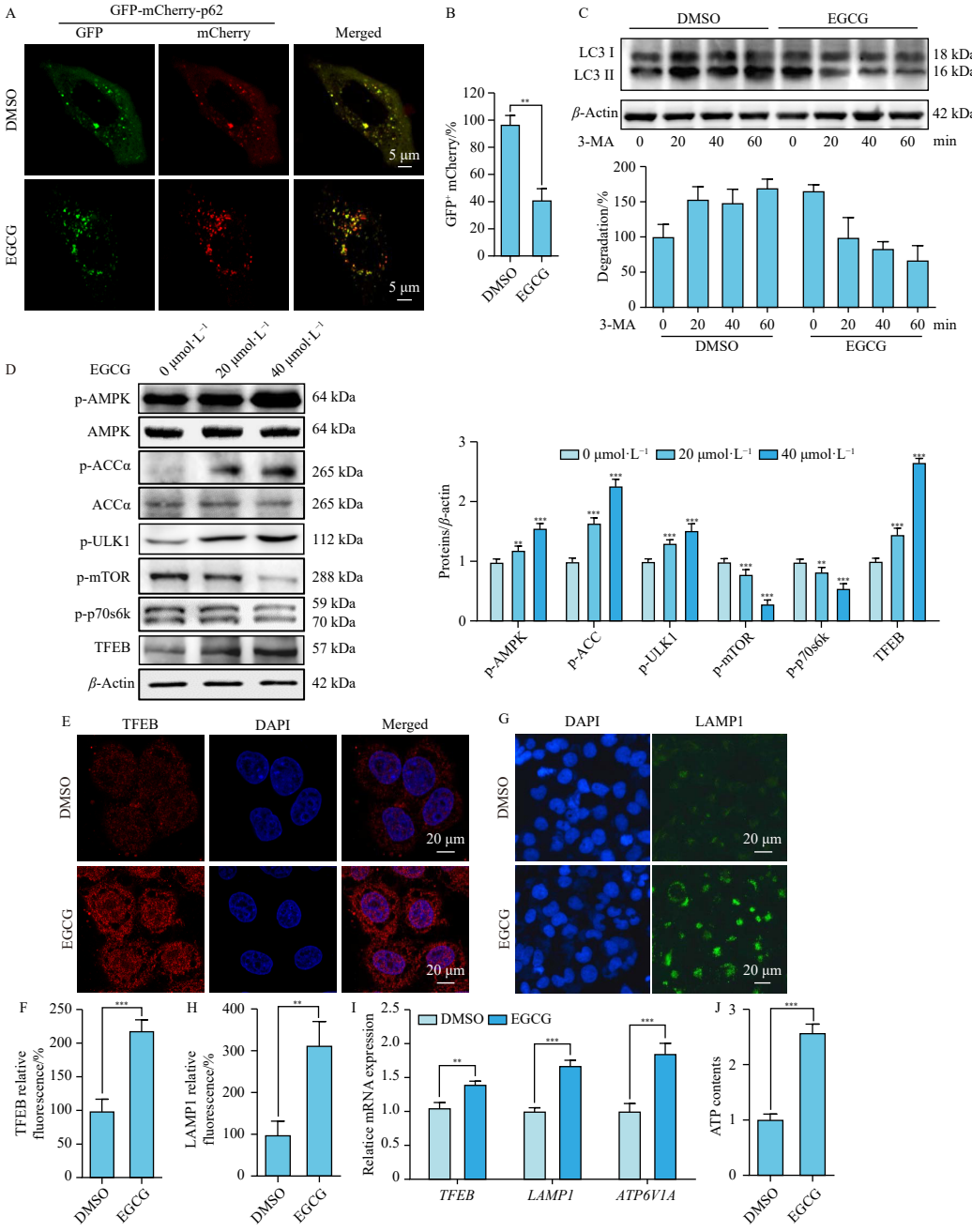

Fig. 4 EGCG activates the AMPK/TFEB signaling pathway and promotes autophagic degradation and lysosome biogenesis. (A, B) HepG2.2.15 cells transfected with the GFP-mCherry-p62 plasmid were treated with DMSO or 40 μmol·L^{-1} EGCG for 24 h. The distributions of mCherry and GFP puncta were examined by confocal microscopy, and the colocalization was analyzed with ImageJ. The quantitative results were presented as means ± SD (n = 30). Scale bars, 5 μm. $^{**}P$ < 0.01. (C) Analysis of the effect of EGCG on the degradation of the formed autophagosome. HepG2.2.15 cells were treated with DMSO or 40 μmol·L^{-1} EGCG for 24 h, then the pI3KC3 inhibitor 3-MA (10 mmol·L^{-1}) was added to stop the formation of new autophagosomes. At the indicated time points (0, 20, 40, 60 min) after 3-MA addition, Western blotting was performed to determine the levels of LC3-II. Lower panel: the immunoblots were scanned and analyzed with ImageJ. The density value from cells without 3-MA and EGCG treatment was set to 100%; bars represent means ± SD (n = 3). (D) Western blotting analysis of the expression of key molecules in the AMPK/mTOR/TFEB signaling pathway in HepG2.2.15 cells following 24 h treatment with different concentrations of EGCG. Quantitative analysis of each protein expression level. The values were presented as means ± SD (n = 3). $^{**}P$ < 0.01, $^{***}P$ < 0.001 *vs* the 0 μmol·L^{-1} group. (E–J) HepG2.2.15 cells were treated with DMSO or 40 μmol·L^{-1} EGCG for 24 h. Cells were fixed, stained with TFEB antibody, and observed by confocal microscopy. The nucleus was stained with DAPI. Scale bars, 10 μm (E). Cells were stained with LAMP1 antibody and observed by fluorescence microscopy. Scale bars, 20 μm (G). The fluorescence signal intensity of TFEB (F) or LAMP1 (H) was analyzed with ImageJ. Values were means ± SD (n = 50). The mRNA levels of *TFEB* and its targeted genes, *LAMP1* and *ATP6V1A*, were determined by qRT-PCR (I). The ATP levels were determined using an ATP content detection kit (J). The values were normalized to the DMSO group and were presented as means ± SD (n = 3). Comparisons in B, F, H, I, and J were performed using t-test, and comparison in D was performed using one-way ANOVA. $^{**}P$ < 0.01, $^{***}P$ < 0.001.

Autophagy serves as a powerful host defense mechanism against viral infections [34]. However, recent studies indicate that autophagy plays a dual role in HBV replication and infection. The early stages of autophagy are activated by HBV and can facilitate its replication, thereby exacerbating liver disease progression [27–29, 35–37], whereas viral components can be degraded through autophagy [31, 38–40]. Thus, different stages of autophagy have distinct implications for the HBV life cycle (Fig. 7). HBV hijacks components of the autophagic pathway to support its survival. For example, the HBV core protein interacts with ATG12 to access the Atg5-12/16L1 elongation complex, which may serve as a platform for nucleocapsid assembly and stability [30]. Hyperphosphorylated core proteins localize to phagophores to participate in pgRNA packaging, and both core and precore proteins associate with autophagic membranes that fuse with multivesicular bodies to form amphisomes [41]. These amphisomes can subsequently fuse with plasma membranes, facilitating the release of mature HBV particles. Moreover, SHBs have been shown to colocalize with the

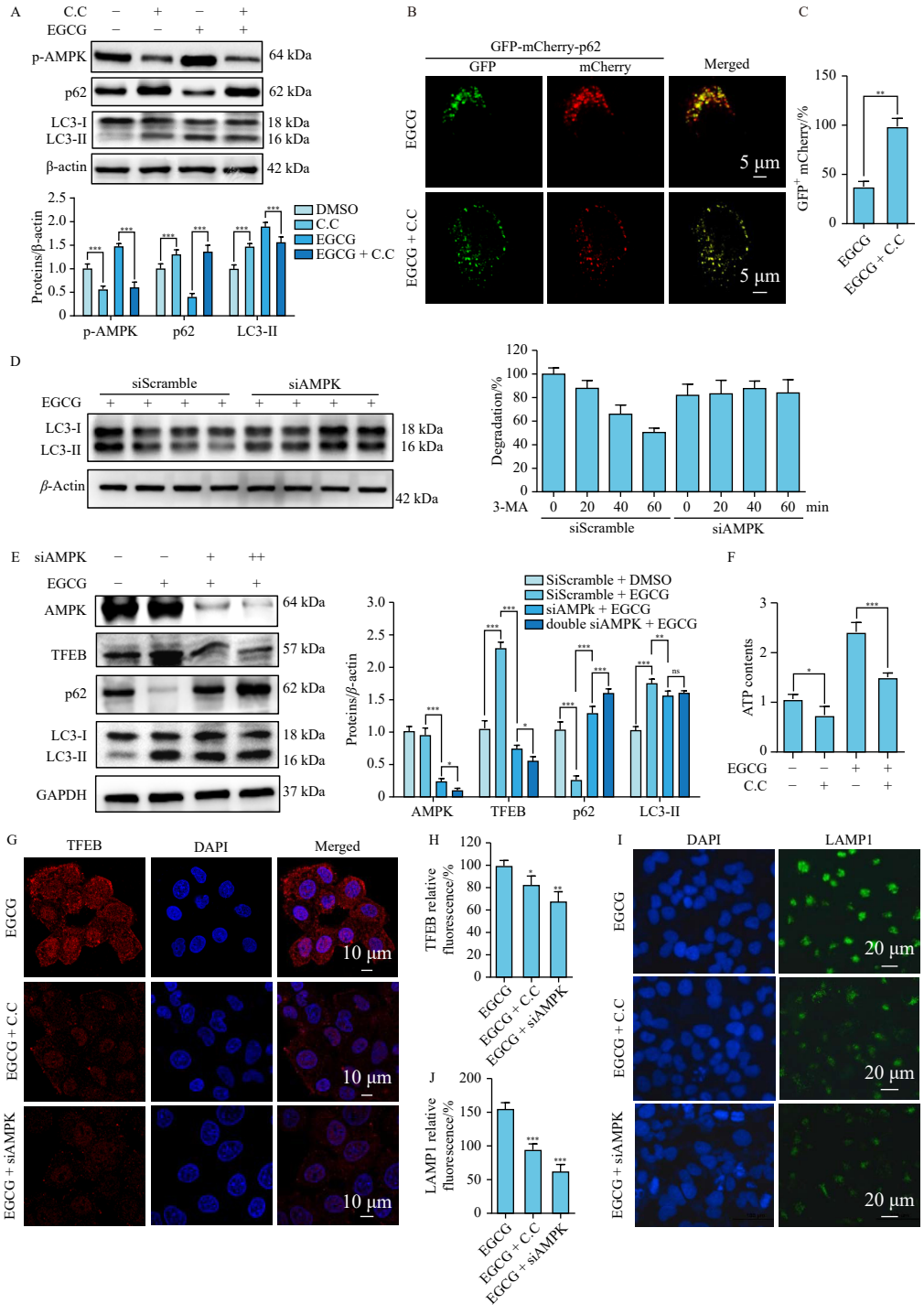

Fig. 5 Inhibition of AMPK suppresses EGCG-induced autophagic degradation and lysosomal biogenesis. (A) HepG2.2.15 cells were treated with DMSO or EGCG (40 μmol·L^{-1}) for 24 h in the absence or presence of AMPK inhibitor C.C (10 μmol·L^{-1}, pretreated for 2 h). The protein levels of p-AMPK, p62, LC3, and p62 in the cell lysates were analyzed *via* Western blotting. The blot bands were quantified by normalization to *β*-actin by ImageJ. Values were means ± SD (n = 3). (B, C) HepG2.2.15 cells transfected with the GFP-mCherry-p62 plasmid were treated with 40 μmol·L^{-1} EGCG for 24 h alone or in combination with C.C (10 μmol·L^{-1}, pretreated for 2 h). Confocal microscopy analysis of the colocalization of mCherry and GFP puncta. Scale bars, 5 μm (B). The mCherry and GFP puncta in cells were quantified with ImageJ. Values were means ± SD (n = 30) (C). (D) HepG2.2.15 cells were transfected with siScramble or siAMPKα pools for 48 h, and then treated with 40 μmol·L^{-1} EGCG. After 24 h, 3-MA (10 mmol·L^{-1}) was added, and the LC3-II levels were analyzed as Fig. 4C described. (E) HepG2.2.15 cells were transfected with siScramble, siAMPKα, or double amounts of siAMPKα for 48 h, and then treated with DMSO or EGCG (40 μmol·L^{-1}) for 24 h. The total protein extracts were subjected to Western blotting. The blot bands were quantified by normalization to GAPDH by ImageJ. Values were means ± SD (n = 3). (F) HepG2.2.15 cells were treated as (A) described. The ATP contents in the cell lysates were determined. The quantitative results were presented as means ± SD (n = 3). (G–J) HepG2.2.15 cells were treated with EGCG (40 μmol·L^{-1}, 24 h) alone, or cotreated with C.C (10 μmol·L^{-1}, pretreated for 2 h), or transfected with siAMPKα for 48 h and then treated with EGCG (40 μmol·L^{-1}, 24 h). Cells were stained with TFEB antibody and observed by confocal microscopy (G). Scale bars, 10 μm (G). Cells were stained with LAMP1 antibody and observed by fluorescence microscopy. Scale bars, 20 μm (I). The fluorescence signal intensity of TFEB (H) or LAMP1 (J) per cell was quantified by normalization to that of the EGCG group with ImageJ. Values were means ± SD (n = 50). Data in C were analyzed using t-test, and other data were analyzed using one-way ANOVA. $^{*}P < 0.05$, $^{***}P < 0.001$, $^{***}P < 0.001$. ns means no significance.

autophagosome marker LC3 during HBV replication, suggesting that the autophagy machinery contributes to HBV envelopment [29]. Collectively, these findings indicate that autophagic membranes are involved in HBV nucleocapsid assembly, trafficking of core and precore proteins, virion envelopment, and viral release. The proviral role of autophagy is supported by our results and previous studies: inhibition of autophagy initiation with 3-MA in our experiments (Fig. 3D), along with silencing of ULK1 or other

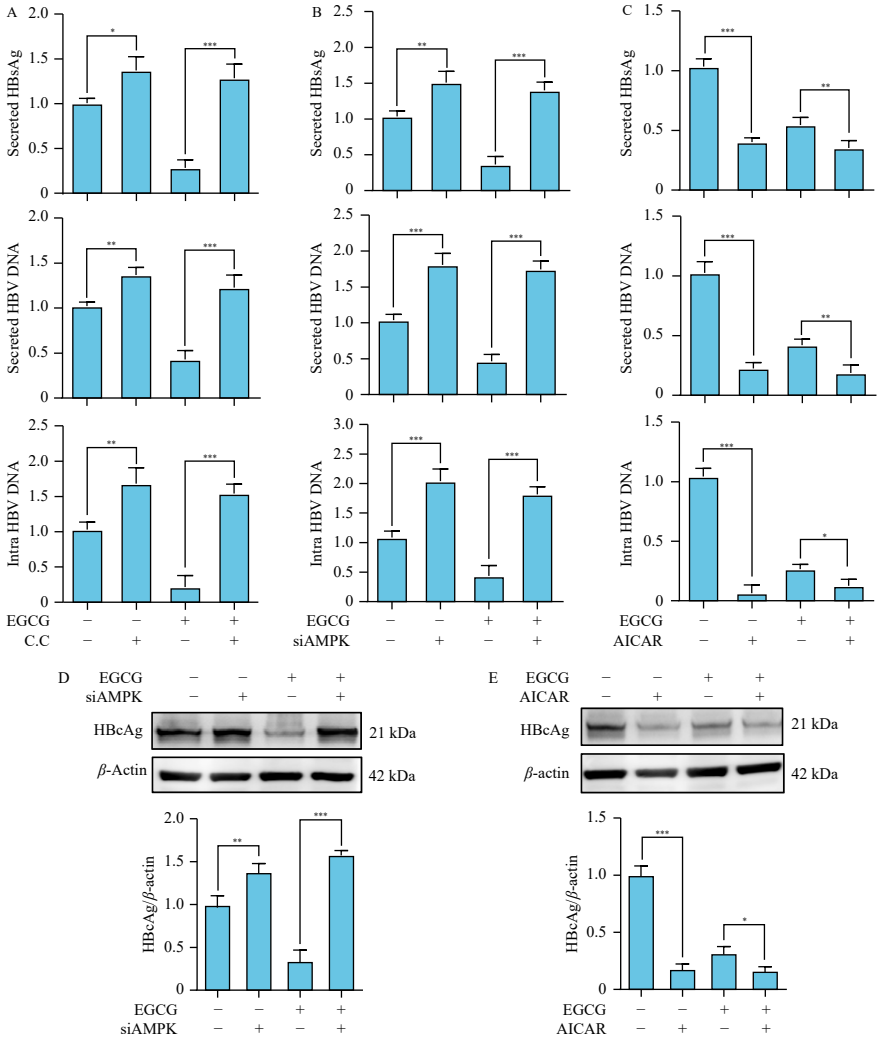

Fig. 6 EGCG inhibits HBV production by activating AMPK to promote the autophagic degradation of the HBV core protein. (A) HepG2.2.15 cells were treated with DMSO or EGCG (40 μmol·L^{-1}) for 24 h in the absence or presence of AMPK inhibitor C.C (10 μmol·L^{-1}, pretreated for 2 h). The three indicators of HBV replication were detected as Fig. 3D described. (B, D) HepG2.2.15 cells were transfected with siScramble or siAMPKα for 48 h, then treated with DMSO or EGCG (40 μmol·L^{-1}) for 24 h, respectively. The three indicators of HBV replication were detected as Fig. 3D described (B). The HBcAg levels in the cell lysates were analyzed *via* Western blotting (D). The quantitative values were normalized to the siScramble + DMSO group and presented as means ± SD (n = 3). (C, E) HepG2.2.15 cells were treated with DMSO or EGCG (40 μmol·L^{-1}) for 24 h in the absence or presence of AMPK activator AICAR (1 mmol·L^{-1}). The three indicators of HBV replication were detected as Fig. 3D described (C). Western blotting analysis of the HBcAg in the cell lysates (E). All values were normalized to the DMSO group and were presented as the means ± SD (n = 3). Data were analyzed using one-way ANOVA. $^{*}P < 0.05$, $^{***}P < 0.001$, $^{***}P < 0.001$.

autophagy-initiating components in prior work, consistently suppressed HBV replication, HBsAg expression, and virion production [42]. Similarly, silencing Beclin1 or ATG5 inhibited HBV replication, while treatment with the autophagy inducer rapamycin (Fig. 3F) or starvation enhanced HBV production [27, 29]. Notably, combining rapamycin with EGCG did not alter the anti-HBV effect of EGCG, despite increased autophagosome formation and LC3-II conversion (Figs. 3G and 3H). Analysis of p62 levels revealed that EGCG markedly reduced p62 compared to rapamycin (Fig. 3H), indicating that EGCG promotes not only autophagosome formation but also autophagic degradation. Therefore, we conclude that autophagic degradation—not autophagosome formation—mediates the inhibitory effect of EGCG on HBV replication. These findings underscore the close association between the HBV life cycle and autophagy: autophagosome membrane elongation supports HBV envelopment and maturation, whereas autophagic degradation limits viral production by degrading viral components (Fig. 7).

Although HBV activates the early autophagic pathway and increases cellular autophagosome levels, it does not stimulate autophagic degradation [14, 27, 43]. This is attributed to the HBx protein impairing lysosomal degradative function [22] and HBV infection reducing Rab7 expression, which hinders autophagosome-lysosome fusion [43]. Conversely, activation of Rab7 and related factors enhances autophagosome-lysosome fusion, promoting the autophagic degradation of HBsAg and HBcAg and thereby suppressing HBV replication and maturation [38]. Consistently, in this study, EGCG treatment enhanced autophagic flux and lysosomal degradative activity, ultimately inhibiting HBV replication and secretion *via* autophagic degradation of the HBV core protein. In contrast, treatment with CQ or bafilomycin A1—two inhibitors that block autophagic degradation by preventing autophagosome-lysosome fusion and lysosomal acidification, respectively—significantly reversed the anti-HBV effect of EGCG and strongly promoted HBV replication and particle release, likely due to enhanced secretory autophagy and expansion of the HBV cccDNA pool. Similarly, studies have shown that 5-FU blocks autophagosome degradation and promotes HBV replication [44], and that inhibition of O-GlcNAcylation prevents autophagosome-lysosome fusion, thereby blocking autophagic degradation of HBV virions and proteins and enhancing viral replication [45]. Clearly, degradative autophagy is detrimental to HBV survival. Recent research provides direct evidence supporting this view: NDP52, an autophagy receptor, restricts HBV replication and secretion by mediating Rab9-

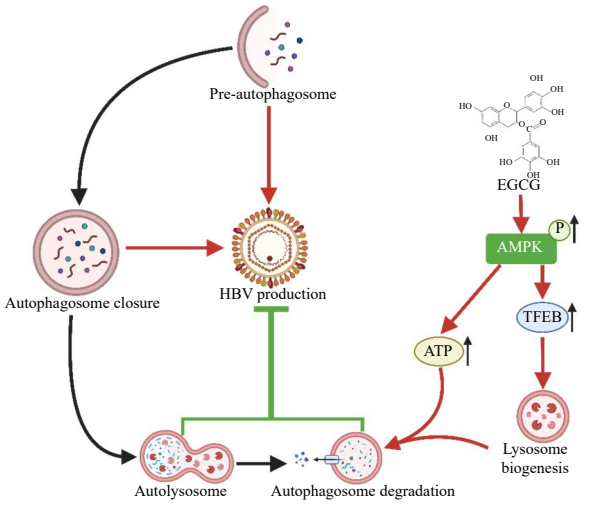

Fig. 7 Diagram showing the proposed mechanism by which EGCG inhibits HBV production through activating the AMPK/TFEB pathway to promote autophagic degradation of viral components. HBV can activate nondegradative autophagy and utilize the pre-autophagosome to promote HBV nucleocapsid assembly, invoke autophagosomes to transport HBV nucleocapsids, and further promote its maturation and secretion. The late autophagy, including autophagolysosome fusion and autophagosome degradation, negatively regulates HBV replication. EGCG can activate AMPK, then promote ATP production and enhance lysosome biogenesis by activating TFEB transcription activity. This process increases autophagy degradation and inhibits HBV replication through the degradation of the HBV core protein.

dependent lysosomal degradation of envelope proteins; likewise, *Galectin-9*, an interferon-stimulated gene, inhibits HBV replication *via* p62/SQSTM1-mediated selective autophagic degradation of core proteins [31, 39]. Together with our findings, these data strongly suggest that autophagic degradation following autophagosome-lysosome fusion represents a major cellular pathway for reducing intracellular HBV loads. Thus, late-stage autophagy—including autophagosome-lysosome fusion and subsequent degradation—negatively regulates HBV production (Fig. 7), potentially by disrupting nucleocapsid stability or the envelopment process through degradation of core or envelope proteins.

Previous studies have demonstrated that EGCG effectively suppresses HBV replication in multiple cell-based models and in human liver chimeric mice [13–17]. Specifically, EGCG inhibits HBV at various stages, including viral entry [16], transcription [46], DNA synthesis [17], and gene expression [47]. Notably, EGCG induces complete autophagy by enhancing lysosomal acidification, revealing a novel anti-HBV mechanism [14]. However, these studies primarily examined long-term effects of EGCG over 3–9 days, and the precise impact of EGCG on the HBV life cycle and its regulation of autophagy and lysosomal acidification remained unclear. To address this, we used HepG2.2.15 cells and 1.3-fold-HBV transiently transfected HuH-7 cells to define the specific steps affected by EGCG. We observed that EGCG treatment rapidly reduced HBV core protein levels within one replication cycle (about 24 h in HepG2.2.15 cells), without altering its transcription, alongside reductions in nucleocapsids and encapsidated pgRNA. We further confirmed that the HBV core protein was degraded *via* EGCG-induced autophagy, consistent with a recent report demonstrating p62/SQSTM1-mediated selective autophagic degradation of HBc [31]. Given that autophagic membranes may mediate trafficking of core proteins or nucleocapsids [41], we propose that autophagy degrades either free core proteins or assembled nucleocapsids—both outcomes would reduce HBV DNA replication. Recently, the role of EGCG-induced autophagy in HBV-related pathologies has gained attention: EGCG alleviates HBV-induced liver injury and fibrosis by promoting autophagic degradation of cytoplasmic high mobility group box 1 (HMGB1) [48].

Our data show that EGCG activates the AMPK/mTOR/ULK1 pathway, initiating autophagy (Fig. 4D). More importantly, AMPK also activates TFEB, as evidenced by its nuclear translocation, increased lysosomal biogenesis, and enhanced autophagic degradation (Figs. 4D–4H). To confirm the essential role of AMPK in EGCG-induced autophagy and its anti-HBV effects, we used the AMPK inhibitor C.C. or AMPK siRNA, both of which significantly reduced TFEB transcriptional activity and the subsequent lysosomal biogenesis and autophagic degradation induced by EGCG (Fig. 5), while increasing HBV production and core protein levels (Figs. 6A, 6B, and 6D). Conversely, co-treatment with the AMPK activator AICAR and EGCG inhibited HBV replication by degrading the core protein, exhibiting greater suppression than EGCG alone (Figs. 6C and 6E). These results demonstrate that AMPK activation promotes autophagic degradation and restricts HBV production, consistent with earlier findings [33]. We also measured ATP production, a known regulator of lysosomal protease activity [33], and found that EGCG significantly increased cellular ATP levels (Fig. 4J). However, AMPK inhibition reversed this effect (Fig. 5F and Fig. S7), indicating that AMPK mediates EGCG-induced ATP production. In this study, we establish that EGCG promotes lysosomal biogenesis and autophagic degradation *via* the AMPK/TFEB pathway. Nevertheless, we do not exclude a potential role for EGCG in autophagosome-lysosome fusion, as TFEB upregulates UVRAG and RAB7 transcription [49], and AMPK contributes to autophagosome maturation and lysosomal fusion [50]. This possibility warrants further investigation.

Moreover, numerous studies indicate that EGCG promotes autophagy in diverse physiological and pathological contexts, including human Tenon's fibroblast transformation, HBV-induced liver injury and fibrosis, and nonalcoholic fatty liver disease [48, 51–54]. However, in hepatoma Hep3B cells, melanoma, cerebral ischemia/reperfusion injury, and models of tumor drug resistance, EGCG inhibits autophagy [18-21]. Additionally, EGCG protects pancreatic β cells from excessive autophagy induced by NR3C1 activation by degrading FTO alpha-ketoglutarate-dependent dioxygenase (FTO) [55]. The reasons for this discrepancy remain unclear and may relate to differences in cell types and EGCG concentrations. For instance, low-dose EGCG (10 μmol·L^{-1}) promotes autophagy and facilitates the degradation of endotoxin-induced HMGB1 aggregates in macrophages, contributing to anti-inflammatory effects [56]. Another study showed that EGCG (10 μmol·L^{-1}) enhances autophagy in vascular endothelial cells by degrading lipid droplets *via* a Ca^{2+}/CaMKKβ/AMPK-dependent mechanism [57]. In contrast, high-dose EGCG (100 μmol·L^{-1}) suppresses autophagy and induces apoptosis in cancer cells and Raw 264.7 macrophages [58, 59]. By adjusting EGCG concentration, a balance between pro- and anti-autophagic effects may be achieved. Given autophagy's critical role in combating HBV and the delicate interplay between its protective and disruptive functions, future studies should investigate whether varying EGCG concentrations exert dual regulatory effects on autophagy during HBV infection.

In vivo, the hepatic microenvironment is highly complex. Stromal cells, such as hepatic stellate cells and endothelial cells, interact with immune cells, including T cells, natural killer (NK) cells, and dendritic cells. For example, activated hepatic stellate cells impair NK cell anti-fibrotic function *via* TGF-β-dependent emperipolesis in HBV cirrhotic patients [60]. These interactions may influence HBV replication, persistence, and immune responses through autophagy. Autophagy regulates the differentiation, development, and homeostasis of immune cells such as monocytes, T cells, and B cells, playing a key role in innate immunity [61]. Suppression of autophagy in neutrophils by HBc or HBe proteins, and induction of autophagy in hepatocytes by HBx, critically regulate HBV replication and persistence [62]. Most investigations into EGCG's effects on HBV-infected cells have been conducted *in vitro*. However, the relevance of these findings to *in vivo* conditions—particularly in infected tissues containing multiple

immune and stromal cell types—remains an active area of research. For instance, EGCG inhibits HBV infection in human liver chimeric mice [15], suggesting that *in vitro* anti-viral effects may translate to *in vivo* settings. EGCG also mitigates lysosomal enzyme release in aged rat livers under a high-cholesterol diet, indicating its role in preserving lysosomal membrane integrity and function *in vivo* [63]—a crucial factor for autophagic degradation. Moreover, EGCG inhibits inflammasome activation in macrophages by promoting autophagic degradation of HMGB1, a pro-inflammatory mediator [48], highlighting its role in modulating immune responses *via* autophagy. Although current mechanistic studies on EGCG and HBV lack comprehensive *in vivo* validation and have limitations, the *in vitro* data provide a solid foundation for future work. Future studies should explore how EGCG regulates HBV replication and autophagic degradation *via* the AMPK/TFEB pathway within the complex hepatic microenvironment.

The complete eradication of HBV remains challenging with current anti-viral therapies (NAs and Peg-IFN) due to the persistence of viral cccDNA in hepatocyte nuclei [64–66]. By limiting cccDNA establishment, EGCG holds promise as part of a combination therapy for HBV-related diseases, complementing conventional treatments that primarily target viral replication. Shifting focus from EGCG's anti-viral properties to its therapeutic effects on HBV-associated pathologies could advance more effective treatment strategies—a key direction for future research. Despite its clinical potential, several challenges must be addressed. A major limitation is EGCG's poor bioavailability and short half-life, which may limit efficacy [67–69]. Therefore, strategies to improve absorption and delivery—such as structural modifications to enhance pharmacokinetics—are essential. Adverse effects of EGCG also warrant attention: cytotoxicity, hepatotoxicity, and nephrotoxicity have been reported with green tea extracts or EGCG supplements [70–72]. Researchers must elucidate the mechanisms underlying these toxicities and establish safe consumption guidelines. Furthermore, translating findings from *in vitro* and animal models to human clinical trials presents significant challenges, necessitating well-designed clinical studies to evaluate EGCG as an adjunct therapy for chronic HBV infection. Exploring combination regimens involving EGCG may yield more effective treatments for HBV-related diseases.

5. Conclusion

Overall, this study demonstrates that EGCG enhances autophagic degradation and lysosomal biogenesis by activating the AMPK/TFEB signaling pathway. This activation mediates the anti-HBV effects of EGCG through promoting autophagic clearance of HBV core proteins and suppressing viral replication. These findings highlight the potential of EGCG as a promising therapeutic agent for HBV infection and provide new insights into the complex interplay between autophagy and the HBV life cycle.

Funding

This work was supported by the National Natural Science Foundation of China (No. 81600470) and the Natural Science Foundation of Shandong Province of China (Nos. ZR2022MC053 and ZR2023MH122).

Supporting information

Supporting information for this work can be obtained by contacting the corresponding authors *via* E-mail.

Declaration of competing interest

These authors have no conflict of interest to declare.

Acknowledgements

We thank Prof. Liu Wei from Zhejiang University School of Medicine for providing us with GFP-LC3 plasmid, GFP-mCherry-LC3 plasmid, GFP-mCherry-p62 plasmid and pcDNA3.0-1.3HBV plasmid. We thank Prof. Chen Zhi from State Key Laboratory for Diagnosis and Treatment of Infectious Diseases, The First Affiliated Hospital, Zhejiang University School of Medicine for providing us with HepG2.2.15 cells and HuH-7 cells.

References

1 Trépo C, Chan HL, Lok A. Hepatitis B virus infection. *Lancet*. 2014;384(9959):2053-2063. https://doi.org/10.1016/S0140-6736(14)60220-8.
2 Iannacone M, Guidotti LG. Immunobiology and pathogenesis of hepatitis B virus infection. *Nat Rev Immunol*. 2022;22(1):19-32. https://doi.org/10.1038/s41577-021-00549-4.
3 Yuen MF, Chen DS, Dusheiko GM, et al. Hepatitis B virus infection. *Nat Rev Dis Primers*. 2018;4:18035. https://doi.org/10.1038/nrdp.2018.35.
4 Alonso S, Guerra AR, Carreira L, et al. Upcoming pharmacological developments in chronic hepatitis B: can we glimpse a cure on the horizon? *BMC Gastroenterol*. 2017;17(1):168. https://doi.org/10.1186/s12876-017-0726-2.
5 Locarnini S, Hatzakis A, Chen DS, et al. Strategies to control hepatitis B: public policy, epidemiology, vaccine and drugs. *J Hepatol*. 2015;62(1 Suppl):S76-86.
6 Revill PA, Chisari FV, Block JM, et al. A global scientific strategy to cure hepatitis B. *Lancet Gastroenterol Hepatol*. 2019;4(7):545-558. https://doi.org/10.1016/S2468-1253(19)30119-0.
7 Li J, Liu S, Zang Q, et al. Current trends and advances in antiviral therapy for chronic hepatitis B. *Chin Med J (Engl)*. 2024;137(23):2821-2832. https://doi.org/10.1097/CM9.0000000000003178.
8 Wong GL, Wong VW, Chan HL. Virus and host testing to manage chronic hepatitis B. *Clin Infect Dis*. 2016;62(Suppl 4):S298-305. https://doi.org/10.1093/cid/ciw024.
9 Ward H, Tang L, Poonia B, et al. Treatment of hepatitis B virus: an update. *Future Microbiol*. 2016;11(12):1581-1597. https://doi.org/10.2217/fmb-2016-0128.
10 Ge F, Yang Y, Bai Z, et al. The role of traditional Chinese medicine in anti-HBV: background, progress, and challenges. *Chin Med*. 2023;18(1):159. https://doi.org/10.1186/s13020-023-00861-2.
11 Zhao W, Li B, Hao J, et al. Therapeutic potential of natural products and underlying targets for the treatment of aortic aneurysm. *Pharmacol Ther*. 2024;259:108652. https://doi.org/10.1016/j.pharmthera.2024.108652.
12 Xing L, Zhang H, Qi R, et al. Recent advances in the understanding of the health benefits and molecular mechanisms associated with green tea polyphenols. *J Agric Food Chem*. 2019;67(4):1029-1043. https://doi.org/10.1021/acs.jafc.8b06146.
13 Pang JY, Zhao KJ, Wang JB, et al. Green tea polyphenol, epigallocatechin-3-gallate, possesses the antiviral activity necessary to fight against the hepatitis B virus replication *in vitro*. *J Zhejiang Univ Sci B*. 2014;15(6):533-539. https://doi.org/10.1631/jzus.B1300307.
14 Zhong L, Hu J, Shu W, et al. Epigallocatechin-3-gallate opposes HBV-induced incomplete autophagy by enhancing lysosomal acidification, which is unfavorable for HBV replication. *Cell Death Dis*. 2015;6(5):e1770. https://doi.org/10.1038/cddis.2015.136.
15 Lai YH, Sun CP, Huang HC, et al. Epigallocatechin gallate inhibits hepatitis B virus infection in human liver chimeric mice. *BMC Complement Altern Med*. 2018;18(1):248. https://doi.org/10.1186/s12906-018-2316-4.
16 Huang HC, Tao MH, Hung TM, et al. (–)-Epigallocatechin-3-gallate inhibits entry of hepatitis B virus into hepatocytes. *Antiviral Res*. 2014;111:100-111. https://doi.org/10.1016/j.antiviral.2014.09.009.
17 He W, Li LX, Liao QJ, et al. Epigallocatechin gallate inhibits HBV DNA synthesis in a viral replication-inducible cell line. *World J Gastroenterol*. 2011;17(11):1507-1514. https://doi.org/10.3748/wjg.v17.i11.1507.
18 Chen L, Ye HL, Zhang G, et al. Autophagy inhibition contributes to the synergistic interaction between EGCG and doxorubicin to kill the hepatoma Hep3B cells. *PLoS One*. 2014;9(1):e85771. https://doi.org/10.1371/journal.pone.0085771.
19 Du BX, Lin P and Lin J. EGCG and ECG induce apoptosis and decrease autophagy *via* the AMPK/mTOR and PI3K/AKT/mTOR pathway in human melanoma cells. *Chin J Nat Med*. 2022;20(4):290-300. https://doi.org/10.1016/S1875-5364(22)60166-3.
20 Wang L, Dai M, Ge Y, et al. EGCG protects the mouse brain against cerebral ischemia/reperfusion injury by suppressing autophagy *via* the AKT/AMPK/mTOR phosphorylation pathway. *Front Pharmacol*. 2022;13:921394. https://doi.org/10.3389/fphar.2022.921394.
21 Meng J, Chang C, Chen Y, et al. EGCG overcomes gefitinib resistance by inhibiting autophagy and augmenting cell death through targeting ERK phosphorylation in NSCLC. *Onco Targets Ther*. 2019;12:6033-6043. https://doi.org/10.2147/OTT.S209441.
22 Liu B, Fang M, Hu Y, et al. Hepatitis B virus X protein inhibits autophagic degradation by impairing lysosomal maturation. *Autophagy*. 2014;10(3):416-430. https://doi.org/10.4161/auto.27286.
23 Liu X, Gao X, Yang Y, et al. EVA1A reverses lenvatinib resistance in hepatocellular carcinoma through regulating PI3K/AKT/p53 signaling axis. *Apoptosis*. 2024;29(7-8):1161-1184. https://doi.org/10.1007/s10495-024-01967-0.
24 Li N, Zhang L, Chen L, et al. MxA inhibits hepatitis B virus replication by interaction with hepatitis B core antigen. *Hepatology*. 2012;56(3):803-811. https://doi.org/10.1002/hep.25608.
25 Liao Z, Gong Z, Wang Z, et al. The degradation of TMEM166 by autophagy

promotes AMPK activation to protect SH-SY5Y cells exposed to MPP. *Cells*. 2022;11(17):2706. https://doi.org/10.3390/cells11172706.
26 Han J, Pan X, Gao Y, et al. Inhibition of hepatitis B virus replication by the internal fragment of hepatitis B core protein. *Virus Res*. 2010;150(1-2):129-134. https://doi.org/10.1016/j.virusres.2010.03.005.
27 Sir D, Tian Y, Chen WL, et al. The early autophagic pathway is activated by hepatitis B virus and required for viral DNA replication. *Proc Natl Acad Sci USA*. 2010;107(9):4383-4388. https://doi.org/10.1073/pnas.0911373107.
28 Tian Y, Sir D, Kuo CF, et al. Autophagy required for hepatitis B virus replication in transgenic mice. *J Virol*. 2011;85(24):13453-13456. https://doi.org/10.1128/JVI.06064-11.
29 Li J, Liu Y, Wang Z, et al. Subversion of cellular autophagy machinery by hepatitis B virus for viral envelopment. *J Virol*. 2011;85(13):6319-6333. https://doi.org/10.1128/JVI.02627-10.
30 Döring T, Zeyen L, Bartusch C, et al. Hepatitis B virus subverts the autophagy elongation complex Atg5-12/16L1 and does not require Atg8/LC3 lipidation for viral maturation. *J Virol*. 2018;92(7):e01513-17. https://doi.org/10.1128/JVI.01513-17.
31 Miyakawa K, Nishi M, Ogawa M, et al. Galectin-9 restricts hepatitis B virus replication *via* p62/SQSTM1-mediated selective autophagy of viral core proteins. *Nat Commun*. 2022;13(1):531. https://doi.org/10.1038/s41467-022-28171-5.
32 Paquette M, El-Houjeiri L, L CZ, et al. AMPK-dependent phosphorylation is required for transcriptional activation of TFEB and TFE3. *Autophagy*. 2021;17(12):3957-3975. https://doi.org/10.1080/15548627.2021.1898748.
33 Xie N, Yuan K, Zhou L, et al. PRKAA/AMPK restricts HBV replication through promotion of autophagic degradation. *Autophagy*. 2016;12(9):1507-1520. https://doi.org/10.1080/15548627.2016.1191857.
34 Choi Y, Bowman JW and Jung JU. Autophagy during viral infection—a double-edged sword. *Nat Rev Microbiol*. 2018;16(6):341-354. https://doi.org/10.1038/s41579-018-0003-6.
35 Ueno T, Komatsu M. Autophagy in the liver: functions in health and disease. *Nat Rev Gastroenterol Hepatol*. 2017;14(3):170-184. https://doi.org/10.1038/nrgastro.2016.185.
36 Gracia-Sancho J, Guixé-Muntet S, Hide D, et al. Modulation of autophagy for the treatment of liver diseases. *Expert Opin Investig Drugs*. 2014;23(7):965-977. https://doi.org/10.1517/13543784.2014.912274.
37 Fu S, Wang J, Hu X, et al. Crosstalk between hepatitis B virus X and high-mobility group box 1 facilitates autophagy in hepatocytes. *Mol Oncol*. 2018;12(3):322-338. https://doi.org/10.1002/1878-0261.12165.
38 Lin Y, Wu C, Wang X, et al. Hepatitis B virus is degraded by autophagosome-lysosome fusion mediated by Rab7 and related components. *Protein Cell*. 2019;10(1):60-66. https://doi.org/10.1007/s13238-018-0555-2.
39 Cui S, Xia T, Zhao J, et al. NDP52 mediates an antiviral response to hepatitis B virus infection through Rab9-dependent lysosomal degradation pathway. *Nat Commun*. 2023;14(1):8440. https://doi.org/10.1038/s41467-023-44201-2.
40 Lin Y, Wu C, Wang X, et al. Synaptosomal-associated protein 29 is required for the autophagic degradation of hepatitis B virus. *FASEB J*. 2019;33(5):6023-6034. https://doi.org/10.1096/fj.201801995RR.
41 Chu JYK, Chuang YC, Tsai KN, et al. Autophagic membranes participate in hepatitis B virus nucleocapsid assembly, precore and core protein trafficking, and viral release. *Proc Natl Acad Sci USA*. 2022;119(30):e2201927119. https://doi.org/10.1073/pnas.2201927119.
42 Lin Y, Deng W, Pang J, et al. The microRNA-99 family modulates hepatitis B virus replication by promoting IGF-1R/PI3K/Akt/mTOR/ULK1 signaling-induced autophagy. *Cell Microbiol*. 2017;19(5):12709. https://doi.org/10.1111/cmi.12709.
43 Zhou T, Jin M, Ding Y, et al. Hepatitis B virus dampens autophagy maturation *via* negative regulation of Rab7 expression. *Biosci Trends*. 2016;10(4):244-250. https://doi.org/10.5582/bst.2016.01049.
44 Yang J, Zheng L, Yang Z, et al. 5-FU promotes HBV replication through oxidative stress-induced autophagy dysfunction. *Free Radic Biol Med*. 2024;213:233-247. https://doi.org/10.1016/j.freeradbiomed.2024.01.011.
45 Wang X, Lin Y, Liu S, et al. *O*-GlcNAcylation modulates HBV replication through regulating cellular autophagy at multiple levels. *FASEB J*. 2020;34(11):14473-14489. https://doi.org/10.1096/fj.202001168RR.
46 Xu J, Gu W, Li C, et al. Epigallocatechin gallate inhibits hepatitis B virus *via* farnesoid X receptor alpha. *J Nat Med*. 2016;70(3):584-591. https://doi.org/10.1007/s11418-016-0980-6.
47 Wang ZY, Li YQ, Guo ZW, et al. ERK1/2-HNF4α axis is involved in epigallocatechin-3-gallate inhibition of HBV replication. *Acta Pharmacol Sin*. 2020;41(2):278-285. https://doi.org/10.1038/s41401-019-0302-0.
48 He M, Chu T, Wang Z, et al. Inhibition of macrophages inflammasome activation *via* autophagic degradation of HMGB1 by EGCG ameliorates HBV-induced liver injury and fibrosis. *Front Immunol*. 2023;14:1147379. https://doi.org/10.3389/fimmu.2023.1147379.
49 Di Malta C, Cinque L, Settembre C. Transcriptional regulation of autophagy: mechanisms and diseases. *Front Cell Dev Biol*. 2019;7:114. https://doi.org/10.3389/fcell.2019.00114.
50 Jang M, Park R, Kim H, et al. AMPK contributes to autophagosome maturation and lysosomal fusion. *Sci Rep*. 2018;8(1):12637. https://doi.org/10.1038/s41598-018-30977-7.
51 Zhang YL, Zhang YQ, Lin HL, et al. Epigallocatechin-3-gallate increases autophagic activity attenuating TGF-β1-induced transformation of human Tenon's fibroblasts. *Exp Eye Res*. 2021;204:108447. https://doi.org/10.1016/j.exer.2021.108447.
52 Niazpour F, Meshkani R. Unlocking the Therapeutic Potential of Autophagy Modulation by Natural Products in Tackling Non-Alcoholic Fatty Liver Disease. *Phytother Res*. 2025;39(5):2357-2373. https://doi.org/10.1002/ptr.8463.
53 Zhou L, Zhong Y, Wang Y, et al. EGCG identified as an autophagy inducer for rosacea therapy. *Front Pharmacol*. 2023;14:1092473. https://doi.org/10.3389/fphar.2023.1092473.
54 Sharma A, Vaghasiya K, Ray E, et al. Targeted pulmonary delivery of the green tea polyphenol epigallocatechin gallate controls the growth of *Mycobacterium tuberculosis* by enhancing the autophagy and suppressing bacterial burden. *ACS Biomater Sci Eng*. 2020;6(7):4126-4140. https://doi.org/10.1021/acsbiomaterials.0c00823.
55 Shao Y, Zhang Y, Zou S, et al. (−)-Epigallocatechin 3-gallate protects pancreatic β-cell against excessive autophagy-induced injury through promoting FTO degradation. *Autophagy*. 2024;20(11):2460-2477. https://doi.org/10.1080/15548627.2024.2370751.
56 Li W, Zhu S, Li J, et al. EGCG stimulates autophagy and reduces cytoplasmic HMGB1 levels in endotoxin-stimulated macrophages. *Biochem Pharmacol*. 2011;81(9):1152-1163. https://doi.org/10.1016/j.bcp.2011.02.015.
57 Kim HS, Montana V, Jang HJ, et al. Epigallocatechin gallate (EGCG) stimulates autophagy in vascular endothelial cells: a potential role for reducing lipid accumulation. *J Biol Chem*. 2013;288(31):22693-22705. https://doi.org/10.1074/jbc.M113.477505.
58 Zhang Y, Yang ND, Zhou F, et al. (−)-Epigallocatechin-3-gallate induces non-apoptotic cell death in human cancer cells *via* ROS-mediated lysosomal membrane permeabilization. *PLoS One*. 2012;7(10):e46749. https://doi.org/10.1371/journal.pone.0046749.
59 Hashimoto K, Sakagami H. Induction of apoptosis by epigallocatechin gallate and autophagy inhibitors in a mouse macrophage-like cell line. *Anticancer Res*. 2008;28(3a):1713-1718.
60 Shi J, Zhao J, Zhang X, et al. Activated hepatic stellate cells impair NK cell anti-fibrosis capacity through a TGF-β-dependent emperipolesis in HBV cirrhotic patients. *Sci Rep*. 2017;7:44544. https://doi.org/10.1038/srep44544.
61 Germic N, Frangez Z, Yousefi S, et al. Regulation of the innate immune system by autophagy: neutrophils, eosinophils, mast cells, NK cells. *Cell Death Differ*. 2019;26(4):703-714. https://doi.org/10.1038/s41418-019-0295-8.
62 Hu S, Liu X, Gao Y, et al. Hepatitis B virus inhibits neutrophil extracellular trap release by modulating reactive oxygen species production and autophagy. *J Immunol*. 2019;202(3):805-815. https://doi.org/10.4049/jimmunol.1800871.
63 Ravindran R, Jaganathan R, Periandavan K. EGCG exerts its protective effect by mitigating the release of lysosomal enzymes in aged rat liver on exposure to high cholesterol diet. *Cell Biochem Funct*. 2020;38(3):309-318. https://doi.org/10.1002/cbf.3490.
64 Liu S, Zhou B, Valdes JD, et al. Serum hepatitis B virus RNA: a new potential biomarker for chronic hepatitis B virus infection. *Hepatology*. 2019;69(4):1816-1827. https://doi.org/10.1002/hep.30325.
65 Guo JT, Guo H. Metabolism and function of hepatitis B virus cccDNA: implications for the development of cccDNA-targeting antiviral therapeutics. *Antiviral Res*. 2015;122:91-100. https://doi.org/10.1016/j.antiviral.2015.08.005.
66 Xia Y, Guo H. Hepatitis B virus cccDNA: formation, regulation and therapeutic potential. *Antiviral Res*. 2020;180:104824. https://doi.org/10.1016/j.antiviral.2020.104824.
67 Wang CC, Xu H, Man GC, et al. Prodrug of green tea epigallocatechin-3-gallate (Pro-EGCG) as a potent anti-angiogenesis agent for endometriosis in mice. *Angiogenesis*. 2013;16(1):59-69. https://doi.org/10.1007/s10456-012-9299-4.
68 Naumovski N, Blades BL, Roach PD. Food inhibits the oral bioavailability of the major green tea antioxidant epigallocatechin callate in humans. *Antioxidants (Basel)*. 2015;4(2):373-393. https://doi.org/10.3390/antiox4020373.
69 Ramesh N, Mandal AKA. Encapsulation of epigallocatechin-3-gallate into albumin nanoparticles improves pharmacokinetic and bioavailability in rat model. *3 Biotech*. 2019;9(6):238. https://doi.org/10.1007/s13205-019-1772-y.
70 Alfke J, Esselen M. Cellular uptake of epigallocatechin gallate in comparison to its major oxidation products and their antioxidant capacity *in vitro*. *Antioxidants (Basel)*. 2022;11(9):1746. https://doi.org/10.3390/antiox11091746.
71 Younes M, Aggett P, Aguilar F, et al. Scientific opinion on the safety of green tea catechins. *EFSA J*. 2018;16(4):e05239. https://doi.org/10.2903/j.efsa.2018.5239.
72 Rasheed NO, Ahmed LA, Abdallah DM, et al. Nephro-toxic effects of intraperitoneally injected EGCG in diabetic mice: involvement of oxidative stress, inflammation and apoptosis. *Sci Rep*. 2017;7:40617. https://doi.org/10.1038/srep40617.